J|A|C|S
ARTICLES
Published on Web 09/20/2002

Direct Synthesis of Gallium Oxide Tubes, Nanowires, and Nanopaintbrushes

Shashank Sharma and Mahendra K. Sunkara*

Contribution from the Department of Chemical Engineering, University of Louisville, Louisville, Kentucky 40292

Received May 28, 2002

Abstract: We demonstrate bulk synthesis of highly crystalline β-gallium oxide tubes, nanowires, and nanopaintbrushes using molten gallium and microwave plasma containing a mixture of monatomic oxygen and hydrogen. Gallium oxide nanowires were 20−100 nm thick and tens to hundreds of micrometers long. Transmission electron microscopy (TEM) revealed the nanowires to be highly crystalline and devoid of any structural defects. Results showed that multiple nucleation and growth of gallium oxide nanostructures could easily occur directly out of molten gallium exposed to an appropriate composition of hydrogen and oxygen in the gas phase. These gallium oxide nanostructures should be of particular interest for optoelectronic devices and catalytic applications.

Introduction

Nanostructures find unique applications in electronics,[1] optoelectronics,[2] and catalysis due to their high surface-to-volume ratio, enhanced material characteristics due to quantum confinement effects, and the high fraction of chemically similar surface sites. Functionalization of these nanostructures can only be achieved and become useful through the synthesis of bulk quantities of defined structures with controlled composition, crystallinity, and morphology. Gallium oxide is a wide band gap material and is of interest due to its interesting bulk properties such as conduction[3] and luminescence.[4] These properties make it a candidate for gas sensing,[5−7] catalytic,[8,9] and optoelectronic device[10] applications. Nanostructures of gallium oxide will be of particular interest for these applications.

Gallium oxide nanowires have been synthesized by several techniques such as physical evaporation,[11−14] arc discharge, and catalyst-assisted methods.[15−17] All of these techniques have been thought to proceed according to two primary mechanisms. The first mechanism involves carbothermal reduction of gallium oxide to produce gas-phase gallium suboxide growth species. The second mechanism relies on transition metal catalyst or evaporated gallium clusters[18] to provide the necessary template for size control of the resulting nanowires.

We recently presented a conceptually different technique, in which low-melting metals (for example, gallium) provide the solvent medium for bulk nucleation and growth of nanowires, thereby eliminating the need for transition metal clusters as growth templates.[19] We illustrated the use of large droplets (millimeter size) or thin gallium films spread on substrates to initiate nucleation with densities greater than $10^{11}/cm^2$. The large number density of the resulting nanowires makes the technique suitable and interesting for large-scale production. We also pointed out that the gas-phase chemistry could be used to manipulate the absolute size, composition, and crystallinity of the nanowires.[19] The only requirement is that the materials of interest should have extremely low solubility and low wetting characteristics with respect to molten gallium. If the solute wets the molten metal, then two-dimensional crystals (platelets) or three-dimensional crystals are more likely to result rather than one-dimensional crystals. We have previously demonstrated this technique of using molten gallium as the growth medium with synthesis of both silicon and carbon nanowires.[20]

* Corresponding author: Phone 502-852-1558; fax 502-852-6355; e-mail mahendra@louisville.edu.

(1) Cui, Y.; Lieber, C. M. *Science* **2001**, *291*, 851.
(2) Alivisatos, A. P. *Science* **1996**, *271*, 933.
(3) Hajnal, Z. J.; Miró, J.; Kiss, G.; Réti, F.; Deák, P.; Herndon, R. C.; Kuperberg, J. M. *J. Appl. Phys.* **1999**, *86*, 3792.
(4) Binet, L.; Gourier, D. *J. Phys. Chem. Solids* **1998**, *59*, 1241.
(5) Ogita, M.; Higo, K.; Nakanishi, Y.; Hatanaka, Y. *Appl. Surf. Sci.* **2001**, *175−176*, 721.
(6) Fleischer, M.; Kornely, S.; Weh, T.; Frank, J.; Meixner, H. *Sensors Actuators B* **2000**, *69*, 205.
(7) Kohl, D.; Ochs, Th.; Geyer, W.; Fleischer, M.; Meixner, H. *Sensors Actuators B* **1999**, *59*, 140.
(8) Petre, A. L.; Auroux, A.; Gélin, P.; Caldararu, M.; Ionescu, N. I. *Thermochim. Acta* **2001**, *379*, 177.
(9) Nakagawa, K.; Kajita, C.; Okumura, K.; Ikenaga, N.-O.; Nishitani-Gamo, M.; Ando, T.; Kobayashi, T.; Suzuki, T. *J. Catal.* **2001**, *203*, 87.
(10) Miyata, T.; Nakatani, T.; Minami, T. *J. Lumin.* **2000**, *87−89*, 1183.
(11) Dai, Z. R.; Pan, Z. W.; Wang, Z. L. *J. Phys. Chem. B* **2002**, *106*, 902.
(12) Gundiah, G.; Govindaraj, A.; Rao, C. N. R. *Chem. Phys. Lett.* **2002**, *351*, 189.
(13) Zhang, H. Z.; Kong, Y. C.; Wang, Y. Z.; Du, X.; Bai, Z. G.; Wang, J. J.; Yu, D. P.; Ding, Y.; Hang, Q. L.; Feng, S. Q. *Solid State Commun.* **1999**, *109*, 677.
(14) Wu, X. C.; Song, W. H.; Huang, W. D.; Pu, M. H.; Zhao, B.; Sun, Y. P.; Du, J. J. *Chem. Phys. Lett.* **2000**, *328*, 5.
(15) Han, W. Q.; Kohler-Redlich, P.; Ernst, F.; Rühle, M. *Solid State Commun.* **2000**, *115*, 527.
(16) Choi, Y. C.; Kim, W. S.; Park, Y. S.; Lee, S. M.; Bae, D. J.; Lee, Y. H.; Park, G.-S.; Choi, W. B.; Lee, N. S.; Kim, J. M. *Adv. Mater.* **2000**, *12*, 746.
(17) Liang, C. H.; Meng, G. W.; Wang, G. Z.; Wang, Y. W.; Zhang, L. D.; Zhang, S. Y. *Appl. Phys. Lett.* **2001**, *78*, 3202.
(18) Chang, K.-W.; Liu, S.-C.; Chen, L.-Y.; Hong, F. C.-N.; Wu, J.-J. *Mater. Res. Soc. Symp. Proc.* **2002**, *703*, 129.
(19) Sunkara, M. K.; Sharma, S.; Miranda, R.; Lian, G.; Dickey, E. C. *Appl. Phys. Lett.* **2001**, *79*, 1546.

10.1021/ja027086b CCC: $22.00

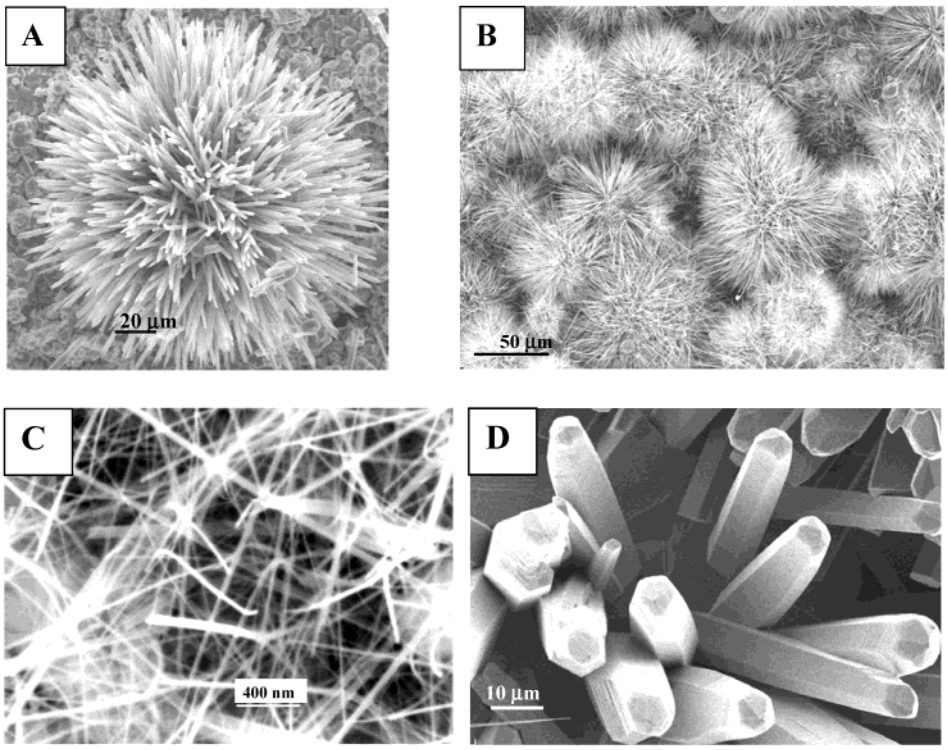

Figure 1. Bulk synthesis of one-dimensional gallium oxide. (A−C) Submicrometer-thick and nanometer-scale gallium oxide rods. (D) Well-faceted micrometer-thick gallium oxide rods synthesized from a large gallium pool and microwave plasma containing atomic oxygen.

In this paper, we demonstrate bulk nucleation and growth of gallium oxide nanostructures directly from molten gallium pools using a microwave oxygen plasma. We foresee that this direct synthesis approach for oxide nanowires could be easily extended to other metals such as aluminum, indium, tin, and zinc. In addition, we present the synthesis of unique geometrical structures of crystalline gallium oxide in the form of tubes and nanopaintbrushes. To date, several geometrical nanostructures have been presented, including spheres,[21] rods,[19] tubes,[22] and belts.[23] In this regard, the synthesis of nanopaintbrushes represents the first of its kind for any inorganic solid. In the case of polymers, self-agglomeration into a structure similar to a nanopaintbrush was reported.[24]

Experimental Section

Synthesis was carried out in a microwave plasma reactor (ASTEX 5010) with $H_2/CH_4/O_2$ gas mixtures. Quartz, alumina, pyrolytic boron nitride, glassy carbon, polycrystalline diamond film, porous graphite, and sapphire substrates were covered with a thin film of molten gallium and were exposed to a microwave plasma containing a range of gas-phase species. During the plasma exposure, molten gallium flowed on all the substrates, forming a thin film, which was followed by formation of a thin polycrystalline film along with sparse nanowires. Gallium droplets were intentionally put on these polycrystalline oxide-covered substrates and further synthesis experiments were carried out. The nanowires and other one-dimensional structures discussed in this paper were grown from these large gallium drops. The substrate temperature was measured by an infrared pyrometer to be approximately 550 °C for 700 W microwave power, 40 Torr total pressure, and 8.0 sccm of O_2 in 100 sccm of hydrogen in the inlet stream. The experiments were performed at the following range of growth conditions: microwave power of 600−1200 W, pressure of 30−60 Torr, growth duration of 1−12 h, 0.6−10 sccm of O_2/0−2 sccm of CH_4 in 100 sccm of hydrogen in the feed gas.

The postsynthesis samples were imaged on a LEO 1430 scanning electron microscope (SEM). As-grown samples were analyzed for crystalline quality by use of a Rigaku powder X-ray diffractometer (XRD). Individual nanowires were analyzed for crystallinity and composition by high-resolution transmission electron microscopy (HRTEM) (200kV JEOL 2010F) and energy-dispersive X-ray spectroscopy (EDX). The samples for TEM analysis were prepared by scraping the nanowire mass from the substrate, dispersing in acetone, and dropping onto a copper TEM grid.

Results and Discussion

Figure 1A−C show SEM images of multiple submicrometer-thick and nanometer-scale gallium oxide needles grown from a large gallium pool. In addition to nanoscale wires, well-faceted one-dimensional structures thicker than 5 μm were also obtained as shown in Figure 1D. The XRD (spectrum not shown) confirmed the as-synthesized sample to be monoclinic gallium oxide phase (a_0 = 12.23 Å, b_0 = 3.04 Å, c_0 = 5.8 Å, β = 103.7°, $C2/m$).[25]

In addition to the nanowires, we obtained nanostructures with paintbrushlike and tubular morphologies on the substrate stage around the substrate that was toward the edge of the dense plasma region (see Figure 2). The individual whiskers have tip diameters ranging from 10 to 100 nm. Table 1 lists the experimental conditions under which different one-dimensional morphologies were obtained. In our current plasma reactor setup, a ball-shaped plasma sits at the center of a circular substrate

(20) Sunkara, M. K.; Sharma, S.; Miranda, R.; Lian, G.; Dickey, E. C. *Mater. Res. Soc. Symp. Proc.* **2002**, *676*, Y.1.6.1.
(21) Kohno, H.; Takeda, S. *J. Cryst. Growth* **2000**, *216*, 185.
(22) Iijima, S. *Nature* **1991**, *354*, 56.
(23) Pan, Z. W.; Dai, Z. R.; Wang, Z. L. *Science* **2001**, *291*, 1947.
(24) Stupp, S. I.; LeBonheur, V.; Walker, K.; Li, L. S.; Huggins, K. E.; Keser, M.; Amstutz, A. *Science* **1997**, *276*, 384.
(25) *Powder Diffraction File Alphabetical Index Inorganic Phases*; International Center for Diffraction Data: Swarthmore, PA, 1989.

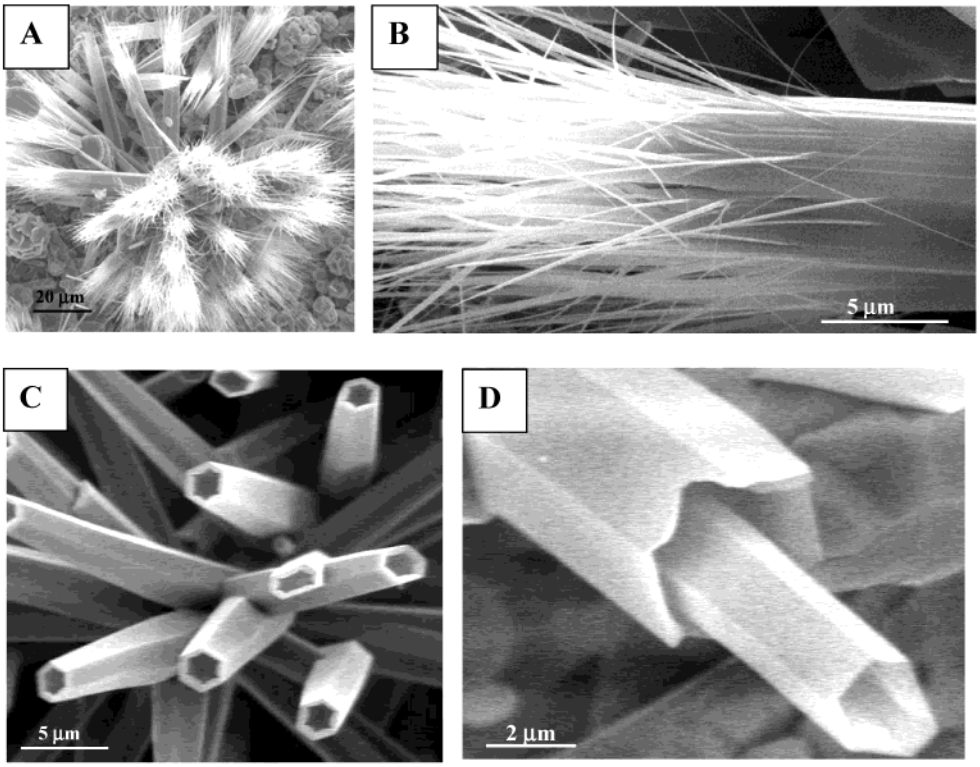

Figure 2. Gallium oxide 1-D structures with interesting morphologies. (A) Cluster of paintbrushlike one-dimensional structures of gallium oxide grown out of a gallium pool. (B) Individual gallium oxide nanopaintbrush. (C, D) Micrometer-scale gallium oxide tubes grown in the same experiment as panels A and B.

Table 1. Summary of Experimental Conditions versus the Resulting One-Dimensional Structures

morphology	flow rate of O_2 in 100 sccm of H_2 (sccm)	microwave power (W)	pressure (Torr)	duration (h)	location on substrate
nanoscale wires	0.6−10	600−900	30−50	1−12	on top of micrometer- to millimeter-sized gallium droplets near center of substrate
micrometer-scale, well-faceted rods	0.6−10	600−900	30−50	1−12	clustered around the micrometer- to millimeter-sized gallium droplets
nanopaintbrushes	7−10	600−1200	30−60	2−10	near edges of substrate
micrometer-scale tubes	7−10	600−1200	30−60	2−10	near edges of substrate

stage, which makes conditions (radical densities) different at different radial positions.

The EDX (spectrum not shown) confirmed that the individual nanowires consist of Ga (Kα at 9.3 keV, Lα at 1.11 eV) and O (Kα at 0.53 keV). Figure 3A shows a bright-field TEM image of a 100-nm-thick nanowire. The HRTEM image in Figure 3B shows a 25-nm-thick gallium oxide nanowire. The lattice spacing in HRTEM image also matched that for bulk β-gallium oxide. The inset in Figure 3B shows the corresponding selected area electron diffraction pattern taken along the [001] zone axis.

The nanowire growth direction was determined to be [110]. Three nanowire samples were examined and the high-resolution TEM results were similar; i.e., structures were devoid of any stacking faults. The absence of stacking faults within the nanowire structures contradicts prior suggestions of structural defect-mediated growth mechanisms for one-dimensional structures.[15] For example, in the case of diamond cubic materials, it was previously suggested that two or more parallel stacking faults are required to form a re-entrant corner for continuous kink creation and step propagation.[26] Typically, the re-entrant corner mediation for growth of a crystal would not necessarily lead to one-dimensional structures.[27] Thus, our present experimental results with nucleation and growth of multiple nanowires from molten gallium suggest a different nucleation and growth phenomenon.

We postulate that the nucleation and growth of oxide nanowires occurs in three basic steps: (1) dissolution of oxygenated gallium species into molten gallium, (2) phase segregation to create multiple nuclei on the surface, and (3) homoepitaxial growth of nuclei into one-dimensional structures from the bottom by use of the dissolved species. The surface dynamics of nuclei on molten gallium, i.e., pattern formation and the time of coalescence, determine if the resulting nanostructure would be a nanowire, tube, or nanopaintbrush. Please refer to the schematic in Figure 4 for illustration of the proposed mechanism.

As depicted in the schematic in Figure 4, the rapid dissolution process results in spontaneous nucleation of nanometer-scale

(26) Angus, J. C.; Sunkara, M.; Sahaida, S. R.; Glass, J. T. *J. Mater. Res.* **1992**, *7*, 3001.
(27) *The Science of Crystallization: Microscopic Interfacial Phenomena*; Tiller, W. A., Ed.; Cambridge University Press: New York, 1991.

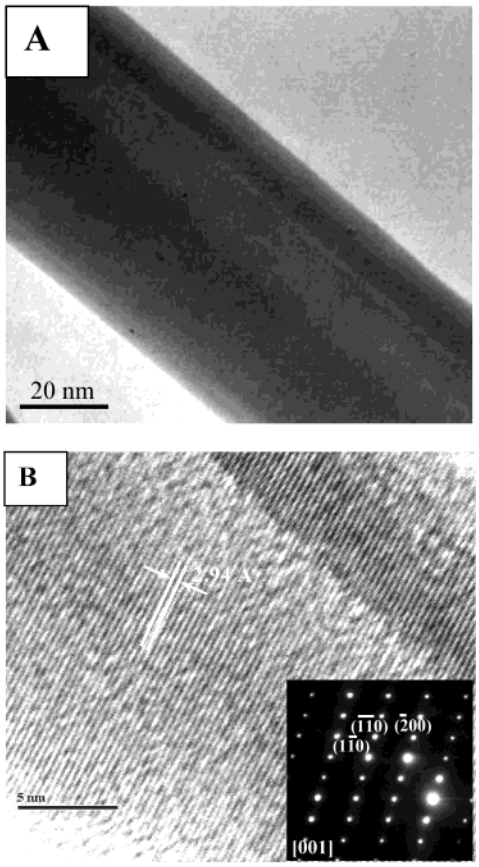

Figure 3. TEM analysis of individual nanowires. (A) Bright-field TEM image of an individual gallium oxide nanowire about 100 nm thick. (B) HRTEM image of a 25 nm thick nanowire. (Inset) Selected area electron diffraction pattern taken along the [001] zone axis.

gallium oxide nuclei on the surface. These surface-segregated nuclei in the absence of redissolution could coalesce on the surface to form a crust. The crust formation prevents further growth of nanometer-scale nuclei in one dimension and leads to a thick, polycrystalline film over molten gallium. Due to poor wettability of gallium oxide with gallium,[28−31] the gallium oxide nuclei surface out but do not propagate laterally, thus ensuring growth in one dimension perpendicular to the molten gallium surface. In the case of hexagonal nuclei formation, lateral growth is probably unavoidable, as these nuclei would propagate parallel to the molten gallium surface, thus eliminating the possibility of growing into a nanowire. This has been observed with plasma nitridation of bulk pools of molten gallium in pure nitrogen environments at substrate temperature of 800 °C or greater.[32,33] In this case, nitrogen plasma exposure resulted in hexagonal, platelet-shaped GaN crystals forming a crust over the molten gallium surface.[32] The resulting crust was found to be highly *c*-plane textured with in-plane orientation between crystals.[33] However, the plasma nitridation of thin gallium films resulted in the growth of gallium nitride nanowires due to the deprived supply of gallium necessary for lateral growth of platelet-shaped crystals.[33] In the present work, hydrogen/oxygen chemistry seems to provide simultaneous dissociation of surface-segregated oxide nuclei to prevent complete crust formation, enabling one-dimensional growth.

The proposed three-step mechanism is further analyzed with thermodynamic arguments and a specific set of experiments. The Gibbs free energies for reactions between both molecular and atomic oxygen species with molten gallium to produce solid gallium oxide are determined to be highly negative, which suggests spontaneity. The estimated nuclei size of gallium oxide nucleation out of molten gallium using classical nucleation theory is predicted to be in the nanometer scale for extremely low partial pressures of oxygen in the vapor phase over molten gallium. This suggests that bulk nucleation of nanometer-scale gallium oxide nuclei by oxygen vapor over a molten gallium pool is thermodynamically feasible. The main question is, however, whether the molten gallium−vapor-phase interaction results in dissolution or in generation of vapor-phase species such as gallium suboxides, gallium hydrides, and pure gallium vapor. The generation of vapor-phase species would lead to eventual loss of gallium from our experiments. In any case, the overall interaction of monatomic oxygen with molten gallium is represented with the following set of reactions. Surface species are denoted with asterisks.

$$Ga_{(l)} + O_{(g)} \leftrightarrows GaO_{(g)} \quad (1)$$

$$2Ga_{(l)} + O_{(g)} \leftrightarrows Ga_2O_{(g)} \quad (2)$$

$$Ga_{(l)} + O_{(g)} \leftrightarrows GaO^* \quad (3)$$

$$2Ga_{(l)} + O_{(g)} \leftrightarrows Ga_2O^* \quad (4)$$

The surface suboxide species from reactions 3 and 4 could undergo dissolution to produce subsurface species and recombination to remove the dissolved oxygen from molten gallium according to

$$Ga_2O^* \leftrightarrows Ga_2O_{(l)} \quad (5)$$

$$2Ga_2O_{(l)} \leftrightarrows 4Ga_{(l)} + O_{2(g)} \quad (6)$$

Reactions 3 and 4 represent chemisorption of oxygen on molten gallium surface, and reactions 5 and 6 represent dissolution of surface species into the bulk and bubbling in gallium pools upon exposure to the plasma, respectively. The diffusion of chemisorbed oxygen complexes versus the thermal desorption determines the solubility of dissolved oxygenated species within molten gallium. The surface diffusion coefficient is typically orders of magnitude higher than the bulk diffusion coefficient. The average lifetime of a surface-adsorbed species is a function of the absolute value of the heat of desorption and temperature.[34]

(28) On the basis of the average values of surface energies for gallium oxide (1.105 J/m^2, determined from heat of sublimation data)[29] and molten gallium (0.718 J/m^2),[30] the contact angle is estimated as 180° by use of the equation of state[31] and Young's equation. Poor wettability of gallium oxide with molten gallium was further confirmed by two different experimental observations. Molten gallium film spread on polycrystalline gallium oxide film was converted into droplets when exposed to microwave plasma containing oxygen and hydrogen radicals for less than 10 min. The second experimental observation was the convex meniscus indicating obtuse contact angle between the gallium oxide rod and the molten gallium at the interface. In theory, other molten metals such as In, Al, Sn, and Zn would also form a convex meniscus with their oxides due to high surface energies.

(29) *CRC Handbook of Chemistry and Physics*; Weast, R. C., Ed.; CRC Press Inc.: Cleveland, OH, 1977.
(30) *The Chemistry of Gallium*; Sheka, I. A., Chaus, I. S., Mityureva, T. T., Eds.; Elsevier: Amsterdam, 1996.
(31) *Applied Surface Thermodynamics*; Neumann, A. W., Spelt, J. K., Eds.; Marcel Dekker Inc.: New York, 1966.
(32) Argoitia, A.; Hayman, C. C.; Angus, J. C.; Wang, L.; Dyck, J. S.; Kash, K. *Appl. Phys. Lett.* **1997**, *70*, 179.
(33) Chandrasekaran, H.; Sunkara, M. K. *Mater. Res. Soc. Symp. Proc.* **2002**, *693*, Y.3.30.1.
(34) *Surface Science: An Introduction*; Hudson, J. B., Ed.; Butterworth-Heinmann: Boston, 1992.

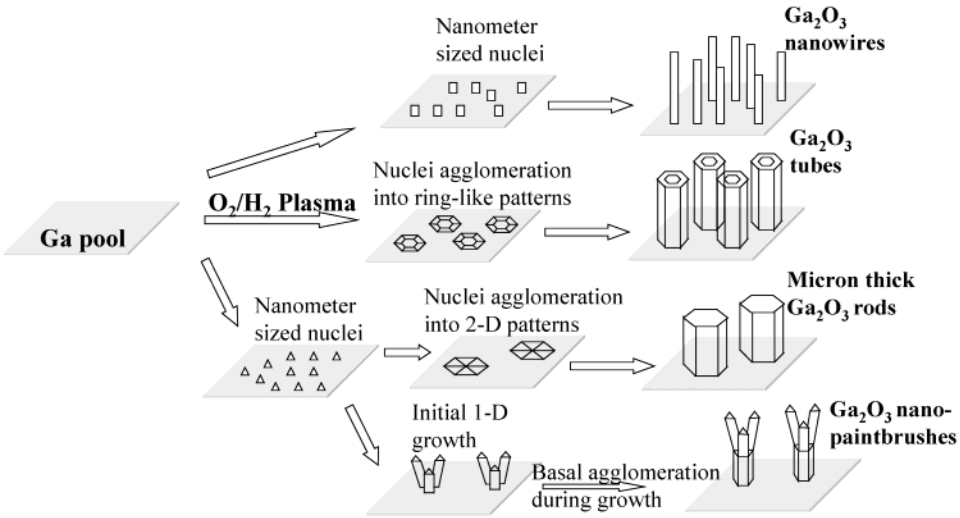

Figure 4. Schematic depicting possible growth routes for multiple nanowires, tubes, and nanopaintbrushes out of a large gallium pool.

Table 2. Minimum Partial Pressures of Monoatomic and Diatomic Oxygen Required for 1-nm-Sized Nuclei of the Respective Oxides at 1000 K[a]

metal	overall formation reaction with atomic oxygen	overall formation reaction with molecular oxygen	minimum partial pressure of O required (Torr)	minimum partial pressure of O_2 required (Torr)
Ga	$2Ga(l) + 3O(g) \rightarrow Ga_2O_3(s)$ [$\Delta G° = 1326.2$ kJ/mol]	$2Ga(l) + {}^3/_2O_2(g) \rightarrow Ga_2O_3(s)$ [$\Delta G° = 763.1$ kJ/mol]	4×10^{-18}	9×10^{-19}
In	$2In(l) + 3O(g) \rightarrow In_2O_3(s)$ [$\Delta G° = 1169.2$ kJ/mol]	$2In(l) + {}^3/_2O_2(g) \rightarrow In_2O_3(s)$ [$\Delta G° = 606.1$ kJ/mol]	2×10^{-16}	2×10^{-15}
Al	$2Al(l) + 3O(g) \rightarrow Al_2O_3(s)$ [$\Delta G° = 1925.2$ kJ/mol]	$2Al(l) + {}^3/_2O_2(g) \rightarrow Al_2O_3(s)$ [$\Delta G° = 1362.1$ kJ/mol]	6×10^{-26}	2×10^{-34}
Sn	$Sn(l) + 2O(g) \rightarrow SnO_2(s)$ [$\Delta G° = 748.2$ kJ/mol]	$Sn(l) + O_2(g) \rightarrow SnO_2(s)$ [$\Delta G° = 372.8$ kJ/mol]	4×10^{-13}	8×10^{-9}
Zn	$Zn(l) + O(g) \rightarrow ZnO(s)$ [$\Delta G° = 435.9$ kJ/ mol]	$Zn(l) + {}^1/_2O_2(g) \rightarrow ZnO(s)$ [$\Delta G° = 248.3$ kJ/mol]	2×10^{-14}	2×10^{-11}

[a] Thermodynamic properties were obtained from ref 36. The estimated Gibbs free energy values for overall reactions are indicated in brackets

At 600 K, the average lifetime of a chemisorbed species such as Ga_2O^* on the molten gallium surface is estimated to be on the order of 1 s, which is 2 and 5 orders of magnitude greater than the characteristic time scales involved with bulk and surface diffusion processes, respectively. A characteristic length scale of 1 μm was assumed. Thus, the surface-adsorbed species are much more likely to undergo diffusion processes, bulk or surface, than desorption into the vapor phase.

Reactions 1 and 2 represent abstraction of gallium by use of atomic oxygen to produce vapor-phase species and represent continuous loss of gallium metal. We performed a set of experiments to track the mass loss of gallium in our experiments with exposure to a plasma containing only oxygen. After several hours of exposure to oxygen plasma, a thin crust was seen on top of the gallium pool with only a negligible change in weight. Complete conversion of gallium to solid gallium oxide would cause a weight increase of approximately 34%. The experimental results showed nominal net loss of mass, indicating that oxygen interaction with molten gallium occurs via a dissolution process much more significantly than chemical vapor transport of gallium by oxide complexes. The thin crust formation and occasional observations of nanowire growth with direct oxygen plasma indicates that hydrogen plays a significant role in preventing crust formation by causing reduction of oxide nuclei to gallium metal. Accordingly, two sets of experiments were performed to observe the interaction of hydrogen plasma with solid gallium oxide and molten gallium. The overall reactions for gallium oxide dissociation are represented in reactions 7 and 8. Both of these reactions could easily be achieved with either molecular or atomic hydrogen.

$$Ga_2O_{3(s)} + 4H_{(g)} \leftrightarrow Ga_2O_{(g)} + 2H_2O \quad (7)$$

$$Ga_2O_{3(s)} + 6H_{(g)} \leftrightarrow 2Ga_{(l)} + 3H_2O \quad (8)$$

The above reactions also compete with the following reactions:

$$Ga_{(l)} + H \leftrightarrow GaH_{(g)} \quad (9)$$

$$Ga_{(l)} + H \leftrightarrow GaH^* \quad (10)$$

$$GaH^* \leftrightarrow GaH_{(l)} \quad (11)$$

$$2GaH_{(l)} \leftrightarrow 4Ga_{(l)} + H_{2(g)} \quad (12)$$

$$H_{(g)} + H_{(g)} \leftrightarrow H_2 \quad (13)$$

The above set of reactions was examined by performing experiments involving hydrogen plasma exposure of molten gallium and solid gallium oxide in separate runs. After several hours of exposure to hydrogen plasma, the gallium oxide solid phase reverted to metallic gallium with a minimal decrease in the total weight. Over different durations of exposure, the mass loss of molten gallium was within 10% of the starting molten gallium mass. This loss in mass is much more than the theoretically estimated weight loss due to gallium vaporization

at the exposure temperatures and pressures. However, the experimentally observed mass loss is much less than the expected mass loss estimated from typical values of gallium abstraction probabilities with hydrogen and the typical process parameters in our flow reactor. From similar abstraction probability values for both hydrogen and oxygen,[35] the mass loss of gallium via abstraction process is estimated to occur at linear rates on the order of tens of milligrams per hour. However, we experimentally observed a constant mass loss of less than 10 mg over the total period of 12-h exposure to hydrogen plasma. In addition, bubbling of molten gallium was observed during microwave plasma treatment. These results indicate that the interaction of monatomic hydrogen with molten gallium occurs with chemisorption followed by dissolution of hydrides as indicated by reactions 11−13. These observations support our hypothesis that hydrogen is responsible for promoting oxide nanowire growth by etching surface-segregated solid gallium oxide nuclei, thus inhibiting the lateral growth of surface nuclei by agglomeration.

The subsequent growth of surface nuclei could occur through attachment kinetics with the suboxide species in the dissolved phase or with gas-phase species. However, our observation of minimal loss in the mass of the solid gallium oxide phase upon exposure to hydrogen plasma indicates that the generation of vapor-phase gallium suboxide species is negligible. This is in contradiction with previously suggested mechanisms for oxide nanowire growth via carbothermal or high-temperature reduction. The nanometer-scale wires showed insignificant tapering from bottom to top, indicating that growth via basal attachment of growth species is more likely than attachment at the tip or at the nanowire perimeter. Micrometer-thick wires clearly exhibited tapering only for short lengths from the top and exhibited faceting at the tips, clearly indicating significant etching at the tip of the micrometer-scale rods.

As shown in the schematic in Figure 4, growth of tubes and paintbrushes can be explained on the basis of initial nucleation and nuclei movement on the molten gallium surface. In some instances, the use of hydrogen in the microwave plasma allowed agglomeration of nanometer-scale surface nuclei into either solid or annular hexagonal patterns. Subsequent attachment of the growth species to solid and annular patterns results in the growth of micrometer-thick hexagonal cross-section solid rods and hexagonal cross-section tubular structures, respectively. Presently, the reason for hexagonal pattern formation is not clear. In the case of agglomeration of neighboring nanometer-scale nuclei at an intermediate stage, the structure evolves into paintbrush morphology. This type of agglomeration could occur due to intermittent changes in the gas phase and temperature that are inherent toward the edge of the plasma discharge. Sequential experiments were performed with the synthesis of nanopaintbrushes and tubular structures. It was observed that, upon extended exposure to the plasma, the one-dimensional structures shown in Figure 2A,D converted to nanometer-scale wires shown in Figure 1A−C. In some instances, the extended exposure to hydrogen/oxygen plasma, the oxide nanostructures developed branching, indicating that secondary nucleation occurred following the hydrogen etching of oxide in the tip region to gallium metal. Our current efforts are focused on determining the agglomeration dynamics of nuclei on molten gallium surface, necessary to control the morphology of resulting nanostructures.

Apart from Ga/Ga_2O_3, we foresee that this direct synthesis technique could be extended to oxide nanostructures of other low-melting metallic systems. As shown in Table 2, extremely low partial pressures of molecular and atomic oxygen are sufficient thermodynamically for creating nanometer-scale nuclei for a variety of other low-melting metallic systems such as Al/Al_2O_3, In/In_2O_3, Sn/SnO_2, and Zn/ZnO. Theoretical estimations of contact angles for these metal oxides with respective molten metals illustrate poor wetting characteristics. Thus, the direct synthesis of nanostructures by appropriate hydrogen/oxygen gas-phase chemistry should be applicable to other important metal-oxide systems.

Conclusions

We have synthesized bulk amounts of highly crystalline gallium oxide tubes, nanowires, and nanopaintbrushes using large gallium pools and a microwave plasma containing atomic oxygen. Direct use of gallium melts in plasma environments allowed bulk synthesis with high nucleation densities and allowed for template-free synthesis of nanostructures with unique geometries. Plasma excitation of the gas phase allowed for synthesis of single-crystal quality nanostructures at much lower temperatures than commonly reported. In addition, the control of gas-phase chemistry allowed the manipulation of the nanostructure composition and morphology. Demonstration of this technique with gallium oxide presents a new route for synthesizing important metal oxides such as indium oxide, tin oxide, and zinc oxide directly from the respective metals.

Acknowledgment. We greatly appreciate partial financial support from the NSF through CAREER grant (CTS 9876251) and an infrastructure grant (EPS 0083103) and the U.S. Air Force through AFO5R Program (F49620-00-1-0310). We also thank Guoda D. Lian at the University of Kentucky for valuable guidance and help with the TEM analysis. We appreciate Dr. John Chaney for helpful editorial comments.

JA027086B

(35) Chabala, J. M. *Phys. Rev. B.* **1992**, *46*, 11346.
(36) *Thermochemical properties of inorganic substances*; Knacke, O., Kubaschewski, O., Hesselman, K., Eds.; Springer-Verlag: New York, 1991.